SOUL in Mouse Eyes Is a New Hexameric Heme-Binding Protein with Characteristic Optical Absorption, Resonance Raman Spectral, and Heme-Binding Properties†

Emiko Sato,‡ Ikuko Sagami,*,‡,§ Takeshi Uchida,|| Akira Sato,|| Teizo Kitagawa,|| Jotaro Igarashi,‡ and Toru Shimizu‡

Institute of Multidisciplinary Research for Advanced Materials, Tohoku University, Sendai 980-8577, Japan, and Okazaki Institute for Integrative Bioscience, National Institutes of Natural Sciences, Okazaki 444-8787, Japan

Received June 17, 2004; Revised Manuscript Received September 1, 2004

ABSTRACT: SOUL is specifically expressed in the retina and pineal gland and displays more than 40% sequence homology with p22HBP, a heme protein ubiquitously expressed in numerous tissues. SOUL was purified as a dimer in the absence of heme from the *Escherichia coli* expression system but displayed a hexameric structure upon heme binding. Heme-bound SOUL displayed optical absorption and resonance Raman spectra typical of 6-coordinate low-spin heme protein, with one heme per monomeric unit for both the Fe(III) and Fe(II) complexes. Spectral data additionally suggest that one of the axial ligands of the Fe(III) heme complex is His. Mutation of His42 (the only His of SOUL) to Ala resulted in loss of heme binding, confirming that this residue is an axial ligand of SOUL. The K_d value of heme for SOUL was estimated as 4.8×10^{-9} M from the association and dissociation rate constants, suggesting high binding affinity. On the other hand, p22HBP was obtained as a monomer containing one heme per subunit, with a K_d value of 2.1×10^{-11} M. Spectra of heme-bound p22HBP were different from those of SOUL but similar to those of heme-bound bovine serum albumin in which heme bound to a hydrophobic cavity with no specific axial ligand coordination. Therefore, the heme-binding properties and coordination structure of SOUL are distinct from those of p22HBP, despite high sequence homology. The physiological role of the new heme-binding protein, SOUL, is further discussed in this report.

Heme plays critical roles in O_2 transport by hemoglobin, O_2 storage by myoglobin, electron transfer by cytochromes, and activation of the O−O bond by P450[1] enzymes and peroxidases (*1*−*3*). New types of heme proteins, designated heme-based sensor proteins (*4*−*6*), have recently been identified. Specifically, heme functions as a sensor, and signals in response to changes in heme electronic and ligand-binding states are transferred to domains that regulate catalytic functions [such as kinase for FixL (*7*, *8*), guanylate cyclase for sGC (*9*, *10*), phosphodiesterase for *Ec* DOS (*11*, *12*), chemotaxis by HemAT (*13*−*15*), and transcription by CooA (*16*, *17*) and NPAS2 (*18*)]. In these proteins, association (or dissociation) of the external gaseous axial ligand such as O_2, NO, or CO to (or from) the heme iron or changes in the heme redox state lead to protein conformational changes in the heme environment, which transmit signals to the other functional domains to initiate catalytic function or DNA binding. In other types of heme-sensing proteins, signals are elicited from the association (or dissociation) of heme per se to (or from) proteins, where transcription or translation are controlled by heme as a ligand for regulatory factors in Bach1 (*19*) or the eukaryotic initiation factor 2a (eIF2a) kinase (HRI) (*20*−*22*), respectively. These proteins sense heme per se and become active (or inactive) upon heme binding. Other intracellular heme-based sensor proteins that exert various unknown important physiological functions remain to be identified.

SOUL, the protein product from a chicken gene, *Soul*, is highly expressed in the retina and pineal gland (*23*). Interestingly, the amino acid sequence of SOUL is similar to that of the heme-binding protein, p22HBP, which was initially purified from mouse liver (*24*). Mouse SOUL has 44% homology to mouse p22HBP at the amino acid level. Molecular analysis of the mammalian and chicken proteins suggests that SOUL and p22HBP are members of a new

† This study was in part supported by Grants-in-Aid from the Ministry of Education, Culture, Sports, Science, and Technology of Japan to I.S. (14580640) and T.K. (14001004) and from the Hayashi Memorial Foundation for Female Natural Scientists to I.S.

* To whom correspondence should be addressed. Phone: +81-75-703-5672. Fax: +81-75-703-5672. E-mail: sagami@kpu.ac.jp.

‡ Tohoku University.

§ Present address: Graduate School of Agriculture, Kyoto Prefectural University, Shimogamo-nakaragi-cho1-5, Sakyo-ku, Kyoto 606-8522, Japan.

|| National Institutes of Natural Sciences.

[1] Abbreviations: P450, cytochrome P450; FixL, an oxygen sensor heme protein from *Rhizobium meliloti*; sGC, soluble guanylate cylase; *Ec* DOS, heme-bound phosophodiesterase from *Escherichia coli* or heme redox sensor from *Escherichia coli*; p22HBP, a heme-binding protein isolated from mammalian liver; HemAT, oxygen sensor heme proteins from *Bacillus subtilis* (HemAT-Bs) and *Halobacterium salinarium* (HemAT-Hs); CooA, a CO-sensing transcription factor from *Rhodospirillum rubrum*; NPAS2, neuronal heme-bound PAS protein from mammals; Bach1, a heme-sensitive transcription regulatory factor; HRI, a heme-sensitive eukaryotic initiation factor 2α kinase; Ni-NTA, nickel nitrilotriacetic acid; CD, circular dichroism; SDS−PAGE, sodium dodecyl sulfate−polyacrylamide gel electrophoresis; CBB, Coomassie Brilliant Blue; BSA, bovine serum albumin; *Sm*FixL, soluble truncated domain of oxygen sensor heme protein from *Sinorhizobium meliloti* (formerly *Rhizobium meliloti*); Hb, hemoglobin; Mb, myoglobin; SwMb, sperm whale myoglobin; hh cyt *c*, horse heart cytochrome *c*; IPTG, isopropyl 1-*β*-thiogalactoside; PMSF, phenylmethanesulfonyl fluoride.

10.1021/bi048742i CCC: $27.50 © 2004 American Chemical Society
Published on Web 10/14/2004

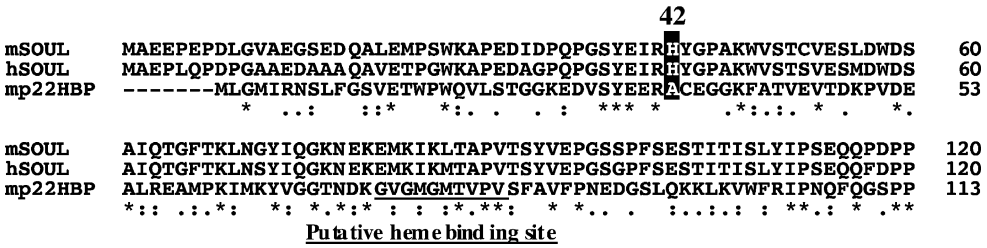

FIGURE 1: Amino acid sequences of SOUL and p22HBP.

protein family. EST database searches further disclose rice, tobacco, and *Arabidopsis* genes with sequence similarity to the SOUL/p22HBP family. On the basis of the observed induction of p22HBP mRNA and protein levels in MEL cells during erythroid differentiation, it is proposed that the p22HBP protein is involved in heme utilization and possibly coupled to hemoglobin synthesis (*24*). Although both mouse SOUL and p22HBP are cytoplasmic proteins, the hydrophobic domain, which is a heme-binding site implied in mouse HBP, human HBP, and chicken SOUL, is absent in mouse and human SOUL (Figure 1). Therefore, we wished to establish whether SOUL binds heme and, if so, to determine its coordination structure to heme compared to that of p22HBP and to further elucidate the role of heme in the functions of these proteins.

In the present study, we developed expression systems of both mouse SOUL and p22HBP proteins in *Escherichia coli* cells and compared the spectral properties of these proteins. Heme-binding studies indicate that SOUL specifically binds one heme per monomer unit and becomes a hexamer upon heme binding. The heme coordination structure and environment of SOUL in terms of optical absorption and resonance Raman spectra of the Fe(III), Fe(II), and Fe(II)−CO complexes are characteristic and distinct from those of p22HBP. Mutagenesis studies were additionally performed to identify the axial ligand of SOUL.

EXPERIMENTAL PROCEDURES

Materials. The expression plasmid of H64Y/V68F apomyoglobin was a kind gift of Dr. John S. Olson. Livers and eyes were obtained from C57BL/6 mice. The mRNA purification and RT-PCR kits were purchased from Amersham Biosciences K. K. (Tokyo, Japan) and Roche Diagnostics K. K. (Tokyo, Japan). Oligonucleotides were synthesized at the Nihon Gene Research Laboratory (Sendai, Japan). The cloning vector, pBluescript SK II(+), and an expression vector, pET28a(+), were purchased from Stratagene (La Jolla, CA) and Novagen (Darmstadt, Germany), respectively. *E. coli* competent XL1-Blue cells (for cloning) and BL21-Codon Plus(RIL) (for protein expression) were purchased from Novagen and Stratagene, respectively. Restriction and modification enzymes for DNA recombination were obtained from Takara Bio Co. (Ohtsu, Japan), Toyobo (Osaka, Japan), New England BioLabs (Beverly, MA), and Roche Diagnostics K. K. Other chemicals purchased from Wako Pure Chemicals (Osaka, Japan) were of the highest quality and were employed without further purification.

Construction of SOUL and p22HBP Expression Plasmids. His-tagged SOUL and p22HBP expression plasmids were generated by subcloning into the pET28a(+) expression vector. The cDNA sequences encoding full-length mouse SOUL and p22HBP were generated by RT-PCR using RNA isolated from mouse eyes and livers, respectively. The primers for RT-PCR are 5′-GCGGATCCATATGGCAGAGGAGCCGGA-3′ and 5′-GGAATTCTTATTTGTTCTCGACGGAG-3′ for SOUL and 5′-GCGGATCCATATGTTGGGCATGATCAG-3′ and 5′-GGAATTCTCATGCCTTCACAAGCCAG-3′ for p22HBP, respectively. The primers for 5′ ends contained *Bam*HI and *Nde*I restriction sites, and those for the 3′ ends contained *Sal*I restriction sites for subcloning. PCR products were digested with *Bam*HI and *Sal*I and inserted into the corresponding sites of the cloning vector, pBluescript SK II(+). The clones obtained were confirmed by determination of the nucleotide sequence by Sanger's method using an automatic sequencer, DSQ-2000L (Shimadzu Co., Kyoto, Japan). pBluescript-SOUL and pBluescript-p22HBP were digested with *Nde*I and *Sac*I and subcloned into the *E. coli* expression vector, pET28a(+), which introduces a 6-His tag at the N-terminus of the desired proteins.

To generate the His42Ala mutant of SOUL, polymerase chain reaction-based mutagenesis was performed with the QuikChange mutagenesis kit from Stratagene, using pET28 containing wild-type SOUL cDNA as a template. Primers employed for mutation were 5′-ATGAGATCCGGGCCTACGGACCGGCTAAG-3′ and 5′-CTTAGCCGGTCCGTAGGCCCGGATCTCAT-3′. The desired substitution was confirmed by sequencing.

Protein Expression and Purification. His-tagged SOUL and p22HBP were expressed in *E. coli* BL21-CodonPlus-(RIL) harboring an expression vector (SOUL/pET28 and p22HBP/pET28, respectively). Protein expression was induced at $OD_{600nm} = 1.2$ for SOUL and $OD_{600nm} = 0.6$ for p22HBP at a final concentration of 0.05 mM IPTG. Cells were further incubated for 20−24 h after IPTG addition. *E. coli* cells expressing SOUL or p22HBP were suspended in buffer A [50 mM sodium phosphate (pH 7.8), 1 mM PMSF, 2 μg/mL aprotinin, 2 μg/mL leupeptin, 2 μg/mL pepstatin, 2 mM 2-mercaptoethanol]. Cells were crushed by pulsed sonication for 2 min (three times at 2 min intervals) on ice using the Ultrasonic Disruptor UD-201 (Tomy Seiko, Tokyo, Japan) and centrifuged at 35000 rpm for 35 min at 4 °C. After centrifugation, ammonium sulfate was added to the resulting supernatant (up to 60% saturation in the case of SOUL). Precipitates were collected and dissolved in buffer A. The solution was passed through a Sephadex G-25 column (4 × 20 cm) preequilibrated with the same buffer. The eluted solution was applied to a Ni-NTA−agarose column preequilibrated with buffer A. In the case of p22HBP, the supernatant was directly applied to a Ni-NTA−agarose column preequilibrated with buffer A. The column was washed sequentially with buffer A containing 20 mM and

50 mM imidazole. SOUL or p22HBP protein was eluted with buffer A containing 100 mM imidazole. Protein fractions were pooled and concentrated. Purified proteins were quickly frozen in liquid nitrogen and stored at −80 °C. Before analysis, the protein buffer was altered to 100 mM Tris-HCl (pH 8.0) containing 0.5 mM EDTA using a Sephadex G-25 column or Bio-Gel P-6 column (Bio-Rad, Hercules, CA). Concentrations were determined using the CBB dye binding method for protein (Nacalai Tesque, Kyoto, Japan) and pyridine hemochromogen method for heme.

Gel Filtration. Gel filtration was performed using an ÄKTA liquid chromatography system equipped with a Superdex75 HR10/30 column or Superdex200 HR10/30 column (Amersham Biosciences). The buffer used for gel filtration contained 100 mM Tris-HCl (pH 8.0) and 0.5 mM EDTA. Molecular masses of protein peaks were estimated relative to those of standard proteins, specifically, thyroglobulin (669 kDa), ferritin (440 kDa), catalase (232 kDa), aldolase (158 kDa), albumin (67 kDa), ovalbumin (43 kDa), chymotrypsinogen A (25 kDa), and ribonuclease A (13.7 kDa).

Optical Absorption and Circular Dichroism (CD) Spectra. Optical absorption spectral experiments under aerobic conditions were performed on Shimadzu UV-2500 and Shimadzu Multi spec 1500 spectrophotometers for samples maintained at 25 °C. CD spectra were obtained with a Jasco J-720 CD spectrometer. To ensure that the temperature of the solution was appropriate, the reaction mixture was incubated for 10 min prior to spectroscopic measurements. Titration experiments were repeated at least three times for each complex. Regression analyses were performed, and lines providing the optimum correlation coefficient were selected.

Resonance Raman Measurements. The Fe(III)SOUL and Fe(III)p22HBP complexes (25 μM in 100 mM Tris-HCl, pH 8.0) were placed in an airtight spinning cell with a rubber septum and reduced by the addition of sodium dithionite at a final concentration of 10 mM. $^{12}C^{16}O$ or $^{13}C^{18}O$ (Shoko, Tokyo, Japan) gas was introduced into the Raman cell with an airtight syringe. Raman scattering was excited at 413.1 nm with a Kr ion laser (Spectra Physics, BeamLok 2060). The excitation light was focused into the cell at a laser power of 5 mW for the Fe(II) and Fe(III) complexes and 0.1−0.2 mW for the Fe(II)−CO complexes to avoid photolysis. Raman spectra were detected with a N_2-cooled CCD camera (Princeton Instruments, CCD-1100PB) attached to a single polychromator (Ritsu Ohyo Kogaku; model DG-1000). The resonance Raman spectra of CO-photolyzed products of the Fe(II)−CO SOUL complex were measured using a 435.7 nm pulse with 10 ns width. The laser pulse was generated by the H_2-first anti-Stokes shift of the second harmonic output of a Nd:YAG laser (Quanta-Ray, LAB-130), which produced 100 mJ pulses at 30 Hz. The laser power was reduced to 80 μJ using a neutral density filter. Raman shifts were calibrated with indene, CCl_4, and an aqueous solution of ferrocyanide.

Stopped-Flow Experiments. Stopped-flow absorbance measurements were conducted using Unisoku RPS-1000 stopped-flow apparatus maintained at 25 °C. Association of CO-heme with apo-SOUL was monitored by measuring the increase in absorbance at 419 nm after mixing 160 volumes of apo-SOUL with one volume of CO-heme and sodium dithionite in 50 mM Tris-HCl (pH 8.0) containing 150 mM NaCl at 25 °C. A plot of k_{obs} versus concentration of apo-SOUL revealed direct correlation, i.e., a straight line. The k_{on} value for the binding of CO-heme was estimated from the slope. Dissociation of heme from Fe(III)SOUL was monitored as Fe(III)Mb formation by measuring the increase in absorbance at 600 nm in a mixture of Fe(III)SOUL, H64Y/V68F apomyoglobin, 0.6 M sucrose, and potassium phosphate buffer (pH 7.0) at 25 °C (*25*). All experiments were repeated at least three times. We obtained the k_{on} value of binding of the CO−Fe(II) heme complex to SOUL, whereas the k_{off} value for dissociation of Fe(III) hemin from SOUL was obtained according to the method of Hargrove et al. (*25*). Therefore, the K_d values summarized in Table 4 calculated from these k_{on} and k_{off} values may not reflect the correct values for binding of the same heme species to SOUL.

RESULTS

Protein Expression and Purification. His-SOUL and His-p22HBP were expressed in *E. coli* cells and purified as apoproteins in the absence of hemin. The proteins were more than 95% homogeneous, as determined by SDS−PAGE followed by staining with CBB R250 (Figure 2A). To eliminate the His tags, both purified His-SOUL and His-p22HBP were treated with thrombin, and undigested His-tag proteins were removed by Ni-NTA−agarose column chromatography. The yields of SOUL and p22HBP were 33.1 and 55.0 mg/L of culture, respectively. Gel filtration analysis using a Superdex200 HR10/30 column revealed that the SOUL apoprotein is a dimer in solution (Figure 2B and Supporting Information, Figure A), while apo-p22HBP is a monomer (data not shown).

Reconstitution with Hemin and Optical Absorption Spectra. Incubation of apo-SOUL and apo-p22HBP with Fe(III) hemin resulted in Soret peak shifts from 396 to 413 and 402 nm, respectively, suggesting specific heme binding to these proteins. Titration experiments with hemin demonstrated that purified SOUL has a high-affinity binding site per protein with a heme:protein ratio of 0.8 (Supporting Information, Figure B). Quantification of heme by the pyridine hemochromogen method (*26*) confirmed that heme-saturated SOUL contains 0.94 mol of heme/monomer. On the other hand, p22HBP bound 0.96 mol of heme/monomer, in agreement with previously published data (*24*). Gel filtration analyses showed that heme-bound SOUL and p22HBP are hexameric (Figure 2B and Supporting Information, Figure A) and monomeric (data not shown), respectively.

Absorption spectra of the Fe(III), Fe(II), and Fe(II)−CO complexes of reconstituted SOUL are depicted in Figure 3A. Soret absorption maxima of the Fe(III), Fe(II), and Fe(II)−CO forms of SOUL were located at 413, 422, and 418 nm, respectively. Spectral parameters are compared with those of other heme proteins in Table 1. Spectral data of Fe(III)-SOUL indicate the presence of a typical 6-coordinate low-spin heme similar to those of *Ec* DOS (*27*, *28*), cytochrome b_5 (*29*), and cytochrome b_{562} (*29*). The Soret peak position at 413 nm was a little blue-shifted relative to the model, suggesting the presence of 6- and 5-coordinated high-spin complexes as minor species for the Fe(III)SOUL. The optical absorption spectrum of the Fe(II)SOUL complex contained peaks at 422, 527, and 558 nm, signifying the presence of 6-coordinate low-spin heme with a 5-coordinate high-spin

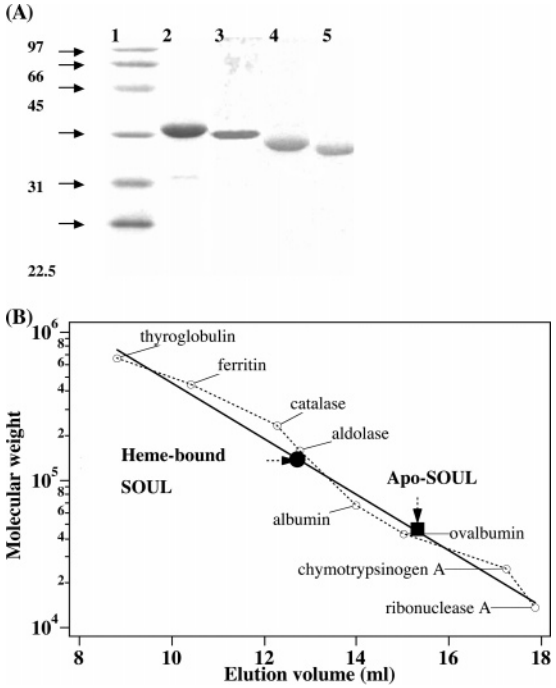

FIGURE 2: Molecular sizes of purified SOUL and p22HBP expressed in *E. coli* cells. (A) SDS−PAGE gel of SOUL and p22HBP stained with CBB R250 including molecular mass marker (lane 1), purified His-tagged SOUL (lane 2), purified SOUL without the His tag (lane 3), purified His-tagged p22HBP (lane 4), and purified p22HBP without the His tag (lane 5). (B) Correlation between the elution volumes of gel filtration and molecular masses of various proteins to estimate the molecular masses of apo-SOUL and heme-binding SOUL.

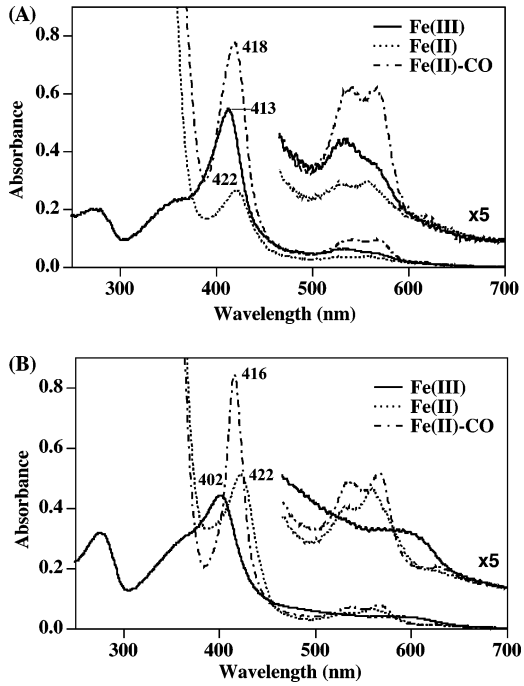

FIGURE 3: Optical absorption spectra of (A) SOUL and (B) p22HBP. Fe(III) (solid line), Fe(II) (dotted line), and Fe(II)−CO (dashed-dashed line) complexes in 50 mM Tris-HCl, pH 8.0.

heme. The presence of these minor species in the Fe(III)-SOUL and Fe(II)SOUL complexes was confirmed by resonance Raman spectra, as described below. The Soret peak of the Fe(II)−CO complex of SOUL was located at 418 nm, but not 450 nm, suggesting that the proximal ligand is likely to be His and not Cys. The peak positions of the SOUL Fe(II)−CO complex are similar to those of heme-bound bovine serum albumin (BSA) (Table 1) (*30*).

Table 1: Optical Absorption Maxima (nm) of SOUL and p22HBP Compared with Other Heme Proteins[a]

protein	Fe(III)	Fe(II)	Fe(II)−CO	ref
SOUL	413, 535, 565	422, 527, 558	418, 536, 563	this work
p22HBP	402, 600	422, 530, 560	416, 537, 567	this work, *24*
Ec DOS	416, 530, 564 (His/H_2O 6cLS)	427, 532, 563 (His/Met 6cLS)	423, 540, 570 (His/CO 6cLS)	*27*, *28*
HRI	418, 538, 564 (?/Cys 6cLS)	428, 530, 560 (His/? 6cLS)	423, 540, 570 (His/CO 6cLS)	*22*
CooA	428, 540, 574 (Cys/Pro 6cLS)	425, 530, 559 (His/Pro 6cLS)	422, 540, 569 (His/CO 6cLS)	*16*, *17*
cyt b_5	412, 533, 562 (His/His 6cLS)	423, 525, 556 (His/His 6cLS)		*29*
cyt b_{562}	418, 530, 564 (His/Met 6cLS)	427, 531, 562 (His/Met 6cLS)	(His/CO 6cLS)	*29*
SwMb	410, 505, 635 (His/H_2O 6cHS)	434, 556 (His 5cHS)	423, 542, 579 (His/CO 6cLS)	*1*
	414, 542, 582 (His/OH^- 6cLS)			*1*
BSA	401, 532, 606	424, 530, 558	419, 538, 567	this work, *30*

[a] Putative coordination structures are noted in parentheses.

On the other hand, the Soret absorption maximum of the Fe(III) p22HBP complex was observed at 402 nm with a broad peak at around 600 nm, suggesting the presence of a 5-coordinate high-spin heme (Figure 3B) (Table 1). Absorption peaks of Fe(II) p22HBP were identified at 422, 530, and 560 nm and those of the Fe(II)−CO complex at 416, 537 and 567 nm. These spectral data of p22HBP are similar to those of SOUL.

To identify the specific axial ligands, the effect of pH modulation on the absorption bands was examined (data not sown). The Soret peak of Fe(III)SOUL at 413 nm remained unchanged between pH 6 and pH 8 but gradually diminished with a peak shift to 390 nm and broadened outside this pH region. In the case of the Fe(II) complex, absorption was not altered between pH 5 and pH 10. The absorbance diminished in the pH region lower than 5, indicating release of heme from the protein.

Resonance Raman Spectra. To further characterize the nature of the heme environment of SOUL, resonance Raman spectra were compared with those of other heme proteins. Resonance Raman spectra of SOUL heme complexes in the high-frequency region are depicted in Figure 4A and summarized in Table 2. Bands at 1373 and 1358 cm^{-1} for the Fe(III) and the Fe(II) complexes of SOUL, respectively, were assigned to redox-sensitive ν_4. In the Fe(III)SOUL complex, the spin- and coordination-state marker band, ν_3, was located at 1504 cm^{-1}, signifying the 6-coordinate low-spin state (Figure 4A). The weak ν_3 bands at 1471 and 1493 cm^{-1} indicated the 6- and 5-coordinate high-spin complexes, respectively, as minor components in Fe(III)SOUL. On the other hand, the ν_3 band in the Fe(II)SOUL complex appeared at 1470 cm^{-1}, which represents a 5-coordinate high-spin complex. A weak band at 1498 cm^{-1} ascribed to a 6-coordinate low-spin complex was additionally observed as a minor component in Fe(II)SOUL. Upon binding of CO to the Fe(II) complex, ν_3 bands shifted to 1499 cm^{-1}, while

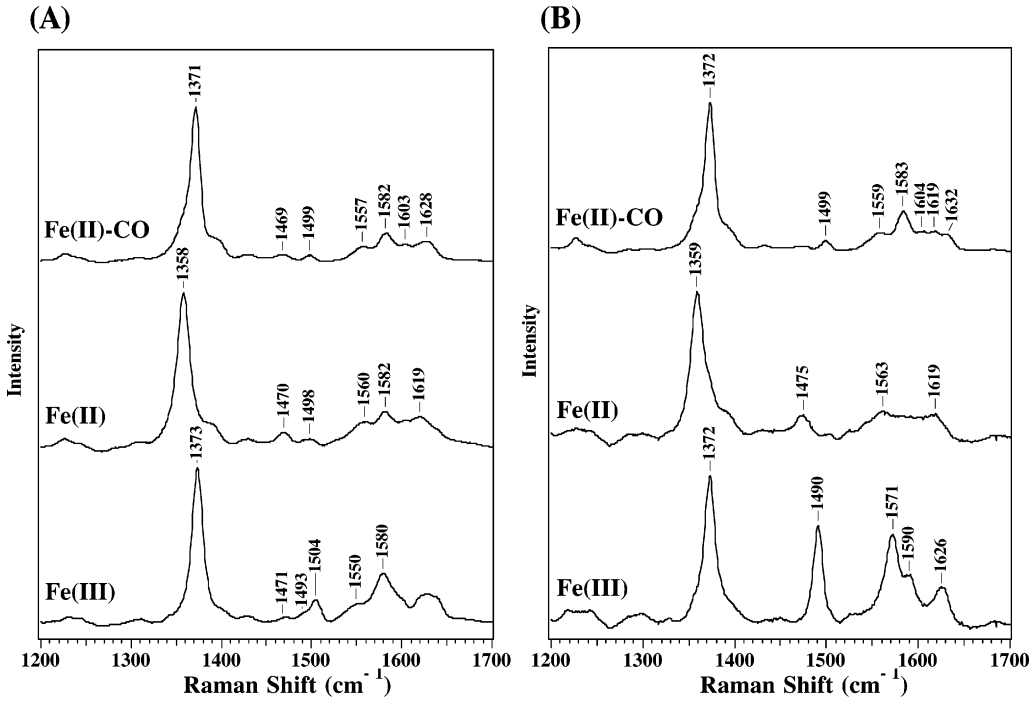

FIGURE 4: Resonance Raman spectra of the high-frequency region of SOUL (A) and p22HBP (B) excited at 413.1 nm in 100 mM Tris-HCl (pH 8.0) buffer.

Table 2: Resonance Raman Data on Fe(III), Fe(II), and Fe(II)−CO Complexes of SOUL and Other Heme Proteins (cm^{-1})

protein		ν_2	ν_3	ν_4	coordination[a]	ref
SOUL	Fe(III)	1580	1504	1373	6cLS	this work
p22HBP	Fe(III)	1571	1490	1372	5cHS	this work
Ec DOS	Fe(III)	1577	1505	1372	6cLS	*34*
CooA	Fe(III)	1585	1504	1375	6cLS	*35*
hh cyt *c*	Fe(III)	1585	1501	1371	6cLS	*36*
SwMb	Fe(III)	1563	1483	1373	6cHS	*37*
SOUL	Fe(II)	1582	1470/1498	1358	5cHS + 6cLS	this work
p22HBP	Fe(II)	1563	1475	1359	5cHS	this work
Ec DOS	Fe(II)	1580	1493	1361	6cLS	*34*
CooA	Fe(II)	1579	1491	1359	6cLS	*38*
hh cyt *c*	Fe(II)	1596	1496	1364	6cLS	*36*
SwMb	Fe(II)	1564	1473	1356	5cHS	*39*
SOUL	Fe(II)CO	1582	1499	1371	6cLS	this work
p22HBP	Fe(II)CO	1583	1499	1372	6cLS	this work
Ec DOS	Fe(II)CO	1581	1496	1370	6cLS	*34*
CooA	Fe(II)CO	1580	1491	1371	6cLS	*35, 38*
SwMb	Fe(II)CO	1585	1501	1373	6cLS	*39*

[a] Abbreviations: 6cLS, 6-coordinate low spin; 5cHS, 5-coordinate high spin; 6cHS, 6-coordinate high spin.

the presence of a band at 1469 cm^{-1} indicated partial photodissociation of CO from the heme. This was accompanied by the weak appearance of ν_4 at 1358 cm^{-1}.

In the case of p22HBP, ν_4 bands of the Fe(III) and the Fe(II) complexes were identified at 1372 and 1359 cm^{-1}, respectively. The ν_3 bands of the Fe(III) and Fe(II) complexes of p22HBP were located at 1490 and 1475 cm^{-1}, respectively, indicating that both complexes are 5-coordinate high spin (Figure 4B). The CO adduct of p22HBP is not as photodissociable as that of SOUL.

The CO-isotope dependences of resonance Raman spectra of the Fe(II)−CO complex of SOUL are illustrated in Figure 5. Spectra a and b in the 350−750 cm^{-1} region in panel A and the 1700−2000 cm^{-1} region in panel B (Figure 5) represent $^{12}C^{16}O$−SOUL and $^{13}C^{18}O$−SOUL, respectively, whereas spectra c in both panels depict the isotope difference (c = a − b). It is evident from the difference spectra that the 497 and 1960 cm^{-1} bands of $^{12}C^{16}O$−SOUL are shifted to 489 and 1868 cm^{-1}, respectively, upon $^{13}C^{18}O$ binding. Accordingly, we assigned the 497 and 1960 cm^{-1} bands to the ν_{Fe-CO} and ν_{C-O} modes, respectively (Table 3). In Figure 5A, the Fe−C−O bending mode, δ_{Fe-C-O}, was also identified at 577 cm^{-1}. Similarly, for the Fe(II)−CO complex of p22HBP, we assigned the 523 and 1959 cm^{-1} bands to the ν_{Fe-CO} and ν_{C-O} modes, respectively (Table 3).

As shown in Figure 6, the ν_{Fe-CO} versus ν_{CO} plot for SOUL falls on the line of the histidine-coordinated heme proteins, while that for p22HBP is off the line, indicating a His−Fe−CO 6-coordinate adduct with SOUL, in contrast to different coordinate structures with p22HBP (presumably the 5-coordinate CO adduct).

The reduced 5-coordinate heme with His as an axial ligand conferred an Fe−His stretching mode (ν_{Fe-His}) in the 200−250 cm^{-1} region (*41*−*43*). However, the Raman spectra of the Fe(II) complex of SOUL with excitation at 413.1, 428.7, and 441.6 nm did not contain a band in this region (data not shown). To characterize the proximal ligand in the Fe(II) complex of SOUL, a resonance Raman spectrum of the photolyzed Fe(II)−CO complex was obtained with 10 ns pulse at 435.7 nm. As shown in Figure 7B, the spectrum of the photolyzed Fe(II)−CO complex displayed ν_3 and ν_4 bands at 1468 and 1353 cm^{-1}, respectively, in the high-frequency region, characteristic of a transient 5-coordinate high-spin Fe(II) complex. In the low-frequency region, an intense band assignable to ν_{Fe-His} was observed at 219 cm^{-1} (Figure 7A), confirming that a ligand of SOUL is neutral His in the Fe(II) complex. The reason for the absence of this band in the spectrum of the stationary state remains to be clarified.

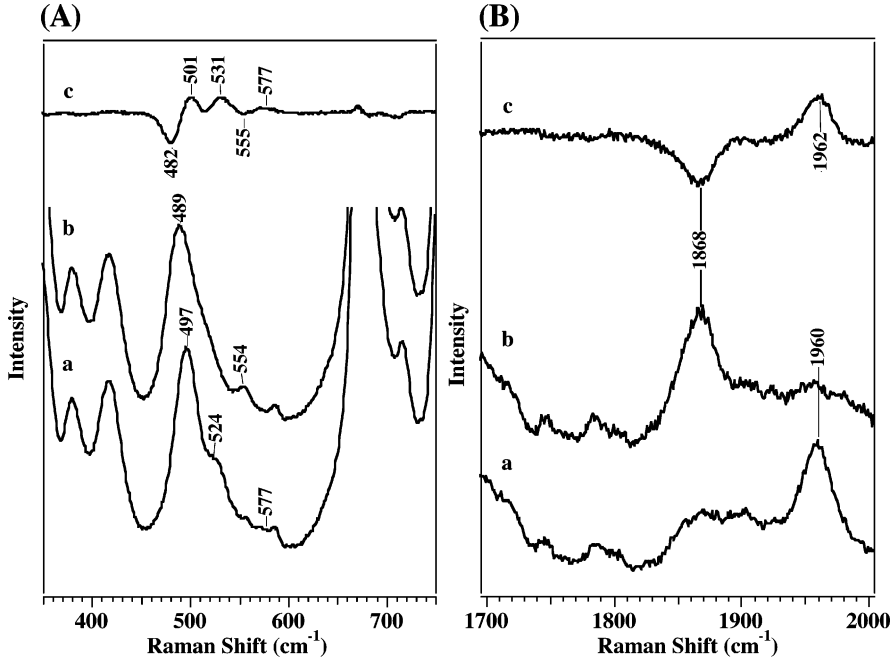

FIGURE 5: Resonance Raman spectra of the Fe(II)−CO complex of SOUL in the low-frequency (A) and high-frequency (B) regions with excitation at 413.1 nm. Spectra of the Fe(II)SOUL complexes of $^{12}C^{16}O$ (a) and $^{13}C^{18}O$ (b) and the difference ($^{12}C^{16}O - {}^{13}C^{18}O$) (c).

Table 3: Comparison of Raman Spectral Frequencies (cm^{-1}) of the Fe(II)CO Complex of SOUL with Those of Other Heme Proteins

protein	ν_{Fe-His}	ν_{Fe-CO}	ν_{C-O}	ref
SOUL	219[a]	497	1960	this work
p22HBP	ND[b]	523	1959	this work
Ec DOS	214[a]	486	1973	*34*
CooA	211[a]	496	1969	*38*
*Sm*FixL*	209	498	1962	*43−45*
sGC	204	473	1987	*46*
SwMb	220	507	1947	*39−41*

[a] Transiently observed immediately after CO photodissociation. [b] Not detected.

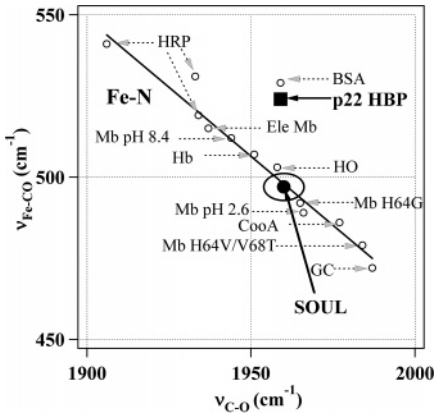

FIGURE 6: Inverse correlation between the ν_{Fe-CO} and ν_{C-O} frequencies. Points denoted with closed circles and squares represent SOUL and p22HBP, respectively. Open circles signify various hemoglobins, myoglobins, peroxidases, and proteins that contain histidine as their proximal ligand, except BSA that has no specific axial ligand for heme.

Mutation at His42. To identify the heme axial ligand of SOUL, His42 (the only His residue in the protein) was mutated to Ala by site-directed mutagenesis. Reconstitution of the H42A mutant with heme resulted in a complex with a small Soret absorption peak at 395 nm, as shown in Figure 8A, suggesting weak nonspecific heme binding. The heme

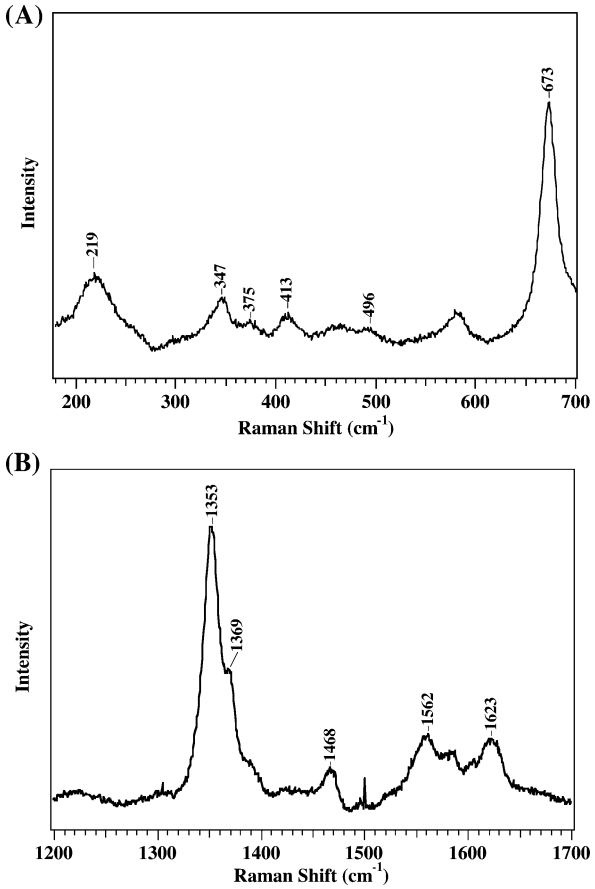

FIGURE 7: Resonance Raman spectra of photolyzed CO adducts of the Fe(II)SOUL complex, using a 10 ns 435.7 nm pulse to both photodissociate the ligand and observe Raman scattering off the sample in the low-frequency (A) and high-frequency (B) regions.

content estimated by the pyridine hemochromogen method was only 0.08 mol/protein, suggesting that His42 is an endogenous ligand for Fe(III)SOUL. This finding was confirmed by resonance Raman spectra. Figure 8B depicts

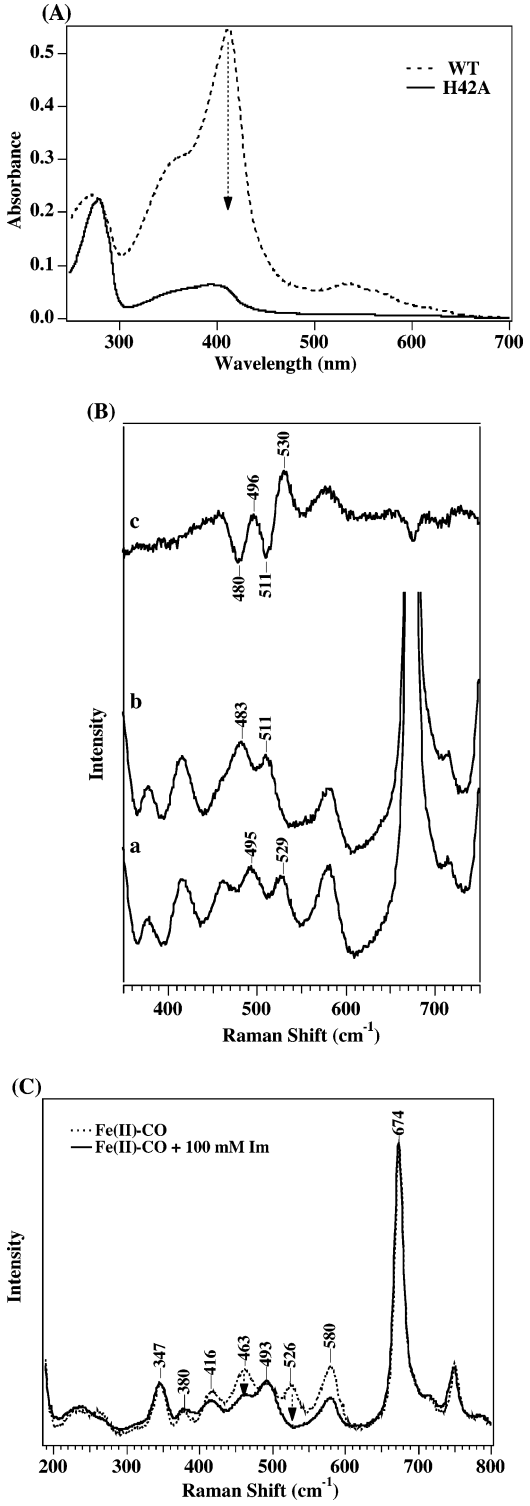

FIGURE 8: Spectral characteristics of the H42A mutant of SOUL. (A) Absorption spectrum of the Fe(III) complex of the H42A mutant. (B) Resonance Raman spectrum of the Fe(II)−CO complex in the low-frequency region with excitation at 413.1 nm. Spectra of the Fe(II)−CO complex of the H42A mutant were obtained with $^{12}C^{16}O$ (a) and $^{13}C^{18}O$ (b). (c) depicts the $^{12}C^{16}O$ minus $^{13}C^{18}O$ difference spectrum. Experimental conditions and spectral assignments are similar to those for Figure 4. (C) Resonance Raman spectra of the Fe(II)−CO complex of the mutant in the absence (dotted line) and presence (solid line) of 100 mM imidazole.

the 413.1 nm-excited resonance Raman spectra of Fe(II) $^{12}C^{16}O$ (a) and $^{13}C^{18}O$ (b) complexes of the H42A mutant in the low-frequency region. Spectrum c represents the $^{12}C^{16}O$ minus $^{13}C^{18}O$ difference. In comparison to wild-type spectra (Figure 5), it is evident that a new ν_{Fe-CO} band for $^{12}C^{16}O$ appears at 529 cm^{-1}, shifts to 511 cm^{-1}, and presumably arises from the 5-coordinate CO complex. This ν_{Fe-CO} band was shifted to 493 cm^{-1} in the presence of exogenous imidazole, as shown in Figure 8C. The frequency is close to that of wild-type SOUL. It appears that exogenous imidazole is bound to the 5-coordinate CO-heme instead of His42 in the His42Ala mutant, while CO occupies the same site as that in the wild-type protein. These data are consistent with our theory that His42 is one of the heme axial ligands for SOUL.

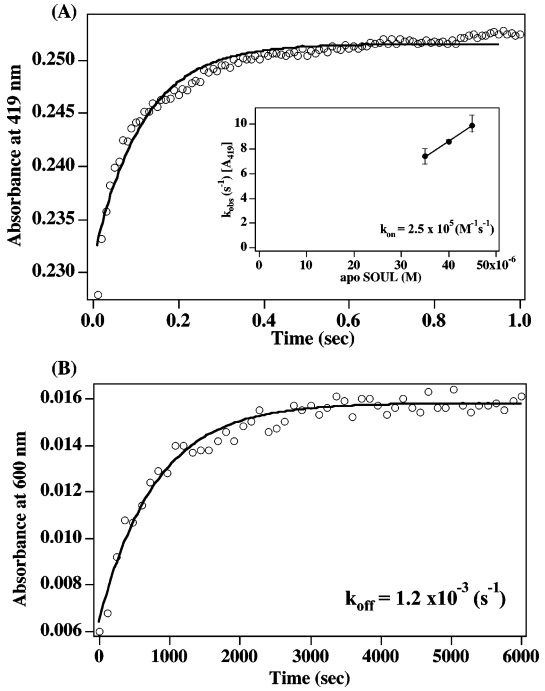

FIGURE 9: Kinetics of heme association (A) and dissociation (B) of SOUL at pH 8.0. (A) Association of CO-heme with apo-SOUL was monitored by measuring the increase in absorbance at 419 nm after mixing using a stopped-flow spectrometer. The inset shows the correlation between k_{obs} and concentration of apo-SOUL. (B) Dissociation of heme from Fe(III)SOUL was monitored as Fe(III)-Mb formation by measuring the increase in absorbance at 600 nm in a mixture of Fe(III)SOUL and H64Y/V68F apomyoglobin (25). Details are provided in Experimental Procedures.

Heme Association and Dissociation Experiments. We obtained association rate constants for binding of the Fe(II)−CO heme complex to apo-SOUL according to the modified methods described by Hargrove et al. (*25*). Fe(II)−CO heme (2−3 μM) was mixed with 30, 35, 40, 45, and 50 μM apo-SOUL using a stopped-flow apparatus at 25 °C. The absorbance at 419 nm increased with a decrease at 408 nm, which was associated with Fe(II)−CO heme binding to SOUL. Fe(II)−CO heme binding to SOUL appeared to be a slow first-order process, as monitored by the increase in absorbance at 419 nm with time (Figure 9A). The rate constant of the association was dependent on the apoprotein concentration (inset in Figure 9A). As summarized in Table 4, the association rate to apo-SOUL was very low, with a k_{on} value of 2.5×10^5 M^{-1} s^{-1}. The k_{on} value of p22HBP was estimated as 2.1×10^8 M^{-1} s^{-1} under similar conditions. We additionally determined the dissociation rate of heme from Fe(III)SOUL and Fe(III)p22HBP by mixing an excess

Table 4: Association and Dissociation Rate Constants and Equilibrium Parameters for Heme Binding to SOUL and Other Heme Proteins

protein	k_{on} (M^{-1} s^{-1})	k_{off} (s^{-1})	K_d (M)	ref
SOUL[a]	2.5×10^5	1.2×10^{-3}	4.8×10^{-9}	this work
p22HBP[a]	2.1×10^8	4.4×10^{-3}	2.1×10^{-11}	this work
SwMb[b]	7.0×10^7	8.4×10^{-7}	1.2×10^{-14}	*25*
BSA[b]	5.7×10^7	7.7	1.4×10^{-7}	*25*

[a] Determined at 25 °C. [b] Determined at 20 °C.

of the H64Y/V68F apomyoglobin mutant (*25*). The reaction was monitored as an increase in absorbance at 410 or 600 nm, accompanied by the formation of Fe(III) heme-bound myoglobin (Figure 9B). The observed k_{off} rates were 1.2×10^{-3} and 4.4×10^{-3} s^{-1} for SOUL and p22HBP, respectively. Table 4 summarizes k_{off} as well as the calculated K_d values for SOUL and p22HBP together with those of other heme-binding proteins. The K_d values of hemin were estimated as 4.8×10^{-9} and 2.1×10^{-11} M for SOUL and p22HBP, respectively.

CD Spectra. From the ultraviolet CD spectrum (Supporting Information, Figure C), the α-helix content of apo-SOUL was estimated as 33% using the CONTINLL program (*44*) [22% with the SELCON3 program (*45*, *46*) and 48% with the CDSSTR (*44*)]. The β-sheet content was estimated as 18% using CONTINLL (33.1% with the SELCON3 program and 23% with CDSSTR). Neither heme binding nor the H42A mutation affected the α-helix and β-sheet content. The Soret CD band of the Fe(III) complex was very weak.

DISCUSSION

Soul was originally isolated by two-tissue suppression subtractive hybridization as a novel chicken gene that is strongly expressed in the retina and pineal gland (*23*). A database search using the chicken SOUL protein sequence also revealed homology with p22HBP isolated from mouse liver (*24*). The search led to the identification of a class of proteins with sequence homology to SOUL and p22HBP in mouse, human, chicken, and zebrafish. Among these, p22HBP is a heme-binding protein with a Soret peak at 402 nm (*24*). To determine the possibility of heme binding to SOUL, we expressed mouse SOUL and p22HBP in *E. coli* cells in the present study. Upon incubation of SOUL with hemin, a Soret band with a peak at 413 nm characteristic of a heme-binding protein with a definite coordination structure was observed, indicating that mouse SOUL is in fact a heme-binding protein. Spectral analyses demonstrate that the SOUL heme coordination environment is distinct from that of p22HBP.

Optical absorption and resonance Raman spectra disclosed that both the Fe(III) and Fe(II) complexes of SOUL are the 6-coordinate low-spin type, while both complexes of p22HBP are the 5-coordinate high-spin type. On the basis of analyses of the His42Ala mutant of SOUL, we propose that His42 is an axial ligand for heme. The Soret band of SOUL for Fe(III) was broad with a peak at 413 nm. The peak position was close to that of the heme complex with water or hydroxyl anion as an axial ligand trans to His, as shown in Table 1. However, we could not confirm the hydroxyl anion as an axial ligand from resonance Raman spectra, since no obvious isotope shift in D_2O was observed for low-frequency modes below 600 cm^{-1} (data not shown). As shown in Table 2, the frequencies of bands assigned for ν_2 are higher for CooA (Cys-Fe-Pro) (*38*) and cytochrome *c* (His-Fe-Met) (*33*) at 1583 and 1585 cm^{-1}, respectively. In the case of Fe(III)-SOUL, the ν_2 band was observed at a lower frequency (1580 cm^{-1}) than the above. Although we cannot exclude the possibility that an increase in the out-of-plane distortion of heme may decrease the frequency of ν_2, these findings suggest that an anionic amino acid is unlikely to be a candidate for the sixth ligand of SOUL. While optical absorption data indicate that the Fe(II)SOUL complex is a 6-coordinate low spin type, the resonance Raman spectrum shows that a 5-coordinate high-spin complex is the major species for the Fe(II)SOUL complex. The reason for this discrepancy is currently unclear. Equilibrium between two species dependent on the protein concentration is possible, since optical absorption spectra are obtained for protein solutions less than 10 μM, while resonance Raman spectra are obtained for solutions more than 25 μM. Similar concentration-dependent coordination changes were observed for heme sensor proteins (*22*).

ν_{Fe-CO} frequencies have a linear inverse correlation with ν_{C-O} frequencies. The ν_{Fe-CO} versus ν_{C-O} plot for SOUL locates on the central part of the line of the histidine-coordinated heme proteins, as shown in Figure 6. This finding indicates that the Fe(II)−CO complex of SOUL contains a neutral His as the proximal ligand trans to CO, and the CO molecule of the complex does not interact strongly with nearby amino acid residues. On the other hand, the ν_{Fe-CO} versus ν_{C-O} plot for p22HBP is off the line but is close to the point of BSA. These data suggest that the CO complex of p22HBP has a five-coordinate CO-heme, similar to BSA.

The ν_{Fe-His} frequencies of sGC (204 cm^{-1}), *Sm*FixL* (209 cm^{-1}), and CooA (211 cm^{-1}) are located at relatively low frequencies (Table 3). On the other hand, the ν_{Fe-His} frequency at 219 cm^{-1} in the Fe(II)SOUL complex is comparable to that in Mb (220 cm^{-1}). The ν_{Fe-His} frequency is sensitive to the hydrogen-bonding status of N_ϵ−H of the coordinated His and the tension imposed on the axial His by the protein moiety. Therefore, the moderate ν_{Fe-His} frequency suggests that a hydrogen bond of Fe(II)SOUL with proximal His is weak, similar to that of Mb. Moreover, the tension on the Fe−His bond is not large, compared with that in CooA and *Sm*FixL*.

The heme-binding rate constant to SOUL was much lower than that of other heme-binding proteins, while dissociation rates were comparable, as shown in Table 4. The calculated K_d value of SOUL (4.8×10^{-9} M) is higher than that of SwMb but lower than that of BSA (*25*). Other heme-binding proteins, such as glutathione *S*-transferase (GST) and HBP23, bind heme with K_d values (10^{-7}−10^{-8} M) similar to that of BSA (*47*−*49*). Accordingly, it is suggested that SOUL has significantly high affinity to heme and is a functional heme protein in cells. We additionally estimated the K_d value of heme for His-tag-free p22HBP (after thrombin digestion) as 2.1×10^{-11} M using a similar method. The K_d value of 2.6×10^{-9} M obtained for GST-fused p22HBP (*24*) by titration with ^{55}Fe heme is 2 orders higher than those obtained in this study. Similarly, the K_d value obtained for tag-free p22HBP using the fluorescence quenching method was relatively high (9×10^{-7} M) (*50*). The character and/or quality of proteins with or without the tag, different methods for determination, or other experimental conditions may

contribute to the differences in the K_d value. sGC and a transcription factor, Bach1, that are regulated by heme display K_d values of about 10^{-8} and 10^{-7} M for heme, respectively (*51*, *52*). However, these values were obtained using other methods and are thus not comparable with the data obtained for SOUL in the present study.

The physiological functions of the SOUL/p22HBP family in cells are currently unknown. A heme-binding protein, HBP23, isolated from rat liver is a member of the peroxiredoxin family of peroxidases (*48*). We examined the peroxidase activities of p22HBP and SOUL by monitoring consumption of H_2O_2. However, the turnover numbers of p22HBP and SOUL were only 2.2% and 3.2% that of horseradish peroxidase, respectively, suggesting that both proteins do not serve as peroxidase in cells. The p22HBP mRNA is ubiquitously expressed in various tissues and extremely abundant in liver (*24*). It is reported that p22HBP is induced during erythroid differentiation and the presence of antisense oligonucleotides decreases heme biosynthesis in dimethyl sulfoxide-induced mouse erythroleukemia cells, indicating that the protein may be involved in heme utilization for heme protein synthesis (*24*). On the other hand, SOUL is specifically expressed in mammalian retina and pineal gland (*23*). Heme proteins such as sGC (*53*), heme oxygenase (*54*), and cytochrome P450s (*55*) have been isolated from these tissues. Therefore, SOUL may play a role in heme transfer to these proteins or bind free heme to protect the retina from damage by reactive oxygen species. It is additionally possible that SOUL functions as a heme sensor by interacting with other proteins. In fact, we identified proteins that specifically bound SOUL from mouse eye cell extracts, depending on the presence of heme (unpublished results). These interacting proteins were not present in liver cell extracts. Further analyses are required to elucidate the functions of SOUL in eye. Interestingly, database analyses revealed that rice, tobacco, and *Arabidopsis* genes have appreciable sequence similarity to the SOUL/HBP family, suggesting that SOUL plays a specific role in plants as well as animals.

ACKNOWLEDGMENT

We thank Dr. John S. Olson (Rice University) for providing us the expression plasmid of H64Y/V68F apomyoglobin.

SUPPORTING INFORMATION AVAILABLE

Gel filtration chromatography patterns of apo-SOUL, heme-bound SOUL, and the H42A mutant, titration of Fe(III) SOUL with different concentrations of heme, and CD spectra in the UV region of apo-SOUL. This material is available free of charge via the Internet at http://pubs.acs.org.

REFERENCES

1. Antonini, E., and Brunori, M. (1971) *Hemoglobin and Myoglobin in Their Reactions with Ligands*, Elsevier/North-Holland Biomedical Press, Amsterdam.
2. Poulos, T. (1988) Heme enzyme crystal structures, *Adv. Inorg. Biochem. 7*, 1−36.
3. Sono, M., Roach, M. P., Coulter, E. D., and Dawson, J. H. (1996) Heme-containing oxygenases, *Chem. Rev. 96*, 2841−2888.
4. Rodgers, K. R. (1999) Heme-based sensors in biological systems, *Curr. Opin. Chem. Biol. 3*, 158−167.
5. Gilles-Gonzalez, M. A. (2001) Oxygen signal transduction, *IUBMB Life 51*, 165−173.
6. Jain, R., and Chan, M. K. (2003) Mechanisms of ligand discrimination by heme proteins, *J. Biol. Inorg. Chem. 8*, 1−11.
7. Dunham, C. M., Dioum, E. M., Tuckerman, J. R., Gonzalez, G., Scott, W. G., and Gilles-Gonzalez, M. A. (2003) A distal arginine in oxygen-sensing heme-PAS domains is essential to ligand binding, signal transduction, and structure, *Biochemistry 42*, 7701−7708.
8. Nakamura, H., Kumita, H., Imai, K., Iizuka, T., and Shiro, Y. (2004) ADP reduces the oxygen-binding affinity of a sensory histidine kinase, FixL: the possibility of an enhanced reciprocating kinase reaction, *Proc. Natl. Acad. Sci. U.S.A. 101*, 2742−2746.
9. Schmidt, P. M., Schramm, M., Schröder, H., Wunder, F., and Stasch, J. P. (2004) Identification of residues crucially involved in the binding of the heme moiety of soluble guanylate cyclase, *J. Biol. Chem. 279*, 3025−3032.
10. Martin, E., Sharina, I., Kots, A., and Murad, F. (2003) A constitutively activated mutant of human soluble guanylyl cyclase (sGC): implication for the mechanism of sGC activation, *Proc. Natl. Acad. Sci. U.S.A. 100*, 9208−9213.
11. Delgado-Nixon, V. M., Gonzalez, G., and Gilles-Gonzalez, M. A. (2000) Dos, a heme-binding PAS protein from *Escherichia coli*, is a direct oxygen sensor, *Biochemistry 39*, 2685−2691.
12. Kurokawa, H., Lee, D. S., Watanabe, M., Sagami, I., Mikami, B., Raman, C. S., and Shimizu, T. (2004) A redox-controlled molecular switch revealed by the crystal structure of a bacterial heme PAS sensor, *J. Biol. Chem. 279*, 20186−20193.
13. Freitas, T. A., Hou, S., and Alam, M. (2003) The diversity of globin-coupled sensors, *FEBS Lett. 552*, 99−104.
14. Zhan, W., and Phillips, G. N., Jr. (2003) Structure of the oxygen sensor in *Bacillus subtilis*: signal transduction of chemotaxis by control of symmetry, *Structure 11*, 1097−1110.
15. Aono, S., Kato, T., Matsuki, M., Nakajima, H., Ohta, T., Uchida, T., and Kitagawa, T. (2002) Resonance Raman and ligand binding studies of the oxygen-sensing signal transducer protein HemAT from *Bacillus subtilis*, *J. Biol. Chem. 277*, 13528−13538.
16. Youn, H., Kerby, R. L., and Roberts, G. P. (2003) The role of the hydrophobic distal heme pocket of CooA in ligand sensing and response, *J. Biol. Chem. 278*, 2333−2340.
17. Aono, S. (2003) Biochemical and biophysical properties of the CO-sensing transcriptional activator CooA, *Acc. Chem. Res. 36*, 825−831.
18. Dioum, E. M., Rutter, J., Tuckerman, J. R., Gonzalez, G., Gillez-Gonzalez, M. A., and McKnight, S. L. (2002) NPAS2: a gas-responsive transcription factor, *Science 298*, 2385−2387.
19. Sun, J., Brand, M., Zenke, Y., Tashiro, S., Groudine, M., and Igarashi, K. (2004) Heme regulates the dynamic exchange of Bach1 and NF-E2-related factors in the Maf transcription factor network, *Proc. Natl. Acad. Sci. U.S.A. 101*, 1461−1466.
20. Rafie-Kolpin, M., Han, A. P., and Chen, J. J. (2003) Autophosphorylation of threonine 485 in the activation loop is essential for attaining eIF2alpha kinase activity of HRI, *Biochemistry 42*, 6536−6544.
21. Inuzuka, T., Yun, B. G., Ishikawa, H., Takahashi, S., Hori, H., Matta, R. L., Ishimori, K., and Morishima, I. (2004) Identification of crucial histidines for heme binding in the N-terminal domain of the heme-regulated eIF2alpha kinase, *J. Biol. Chem. 279*, 6778−6782.
22. Igarashi, J., Sato, A., Kitagawa, T., Yoshimura, T., Yamauchi, S., Sagami, I., and Shimizu, T. (2004) Activation of heme-regulated eukaryotic initiation factor 2alpha kinase by nitric oxide is induced by the formation of a five-coordinate NO-heme complex: optical absorption, electron spin resonance, and resonance Raman spectral studies, *J. Biol. Chem. 279*, 15752−15762.
23. Zylka, M. J., and Reppert, S. M. (1999) Discovery of a putative heme-binding protein family (SOUL/HBP) by two-tissue suppression subtractive hybridization and database searches, *Brain Res. Mol. Brain Res. 74*, 175−181.
24. Taketani, S., Adachi, Y., Kohno, H., Ikehara, S., Tokunaga, R., and Ishii, T. (1998) Molecular characterization of a newly identified heme-binding protein induced during differentiation of urine erythroleukemia cells, *J. Biol. Chem. 273*, 31388−31394.
25. Hargrove, M. S., Barrick, D., and Olson, J. S. (1996) The association rate constant for heme binding to globin is independent of protein structure, *Biochemistry 35*, 11293−11299.
26. Klatt, P., Schmidt, K., Werner, E. R., and Mayer, B. (1996) Determination of nitric oxide synthase cofactors: heme, FAD, FMN, and tetrahydrobiopterin, *Methods Enzymol. 268*, 358−365.

27. Sasakura, Y., Hirata, S., Sugiyama, S., Suzuki, S., Taguchi, S., Watanabe, M., Matsui, T., Sagami, I., and Shimizu, T. (2002) Characterization of a direct oxygen sensor heme protein from *Escherichia coli*. Effects of the heme redox states and mutations at the heme-binding site on catalysis and structure, *J. Biol. Chem. 277*, 23821−23827.
28. Hirata, S., Matsui, T., Sasakura, Y., Sugiyama, S., Yoshimura, T., Sagami, I., and Shimizu, T. (2003) Characterization of Met95 mutants of a heme-regulated phosphodiesterase from *Escherichia coli*. Optical absorption, magnetic circular dichroism, circular dichroism, and redox potentials, *Eur. J. Biochem. 270*, 4771−4779.
29. Mathews, F. S. (2001) in *Handbook of Metalloproteins* (Messerschmidt, A., Huber, R., Poulos, T., and Wieghardt, K., Eds.) Vol. 1, pp 159−171, John Wiley & Sons, Chichester.
30. Rotenberg, M., and Margalit, R. (1985) Deuteroporphyrin-albumin binding equilibrium. The effects of porphyrin self-aggregation studied for the human and the bovine proteins, *Biochem. J. 229*, 197−203.
31. Sato, A., Sasakura, Y., Sugiyama, S., Sagami, I., Shimizu, T., Mizutani, Y., and Kitagawa, T. (2002) Stationary and time-resolved resonance Raman spectra of His77 and Met95 mutants of the isolated heme domain of a direct oxygen sensor from *Escherichia coli*, *J. Biol. Chem. 277*, 32650−32658.
32. Vogel, K. M., Spiro, T. G., Shelver, D., Thorsteinsson, M. V., and Roberts, G. P. (1999) Resonance Raman evidence for a novel charge relay activation mechanism of the CO-dependent heme protein transcription factor CooA, *Biochemistry 38*, 2679−2687.
33. Hu, S. Z., Morris, I. K., Singh, J. P., Smith, K. M., and Spiro, T. G. (1993) Complete assignment of cytochrome *c* resonance Raman spectra via enzymic reconstitution with isotopically labeled hemes, *J. Am. Chem. Soc. 115*, 12446−12458.
34. Hu, S. Z., Smith, K. M., and Spiro, T. G. (1996) Assignment of protoheme resonance Raman spectrum by heme labeling in myoglobin, *J. Am. Chem. Soc. 118*, 12638−12646.
35. Uchida, T., Ishikawa, H., Takahashi, S., Ishimori, K., Morishima, I., Ohkubo, K., Nakajima, H., and Aono, S. (1998) Heme environmental structure of CooA is modulated by the target DNA binding. Evidence from resonance Raman spectroscopy and CO rebinding kinetics, *J. Biol. Chem. 273*, 19988−19992.
36. Takahashi, S., Wang, J., Rousseau, D. L., Ishikawa, K., Yoshida, T., Takeuchi, N., and Ikeda-Saito, M. (1994) Heme-heme oxygenase complex: structure and properties of the catalytic site from resonance Raman scattering, *Biochemistry 33*, 5531−5538.
37. Tamura, K., Nakamura, H., Tanaka, Y., Oue, S., Tsukamoto, K., Nomura, M., Tsuchiya, T., Adachi, S., Takahashi, S., Iizuka, T., and Shiro, Y. (1996) Nature of endogenous ligand binding to heme iron in oxygen sensor FixL, *J. Am. Chem. Soc. 118*, 9434−9435.
38. Rodgers, K. R., Lukat-Rodgers, G. S., and Barron, J. A. (1996) Structural basis for ligand discrimination and response initiation in the heme-based oxygen sensor FixL, *Biochemistry 36*, 9539−9548.
39. Lukat-Rodgers, G. S., and Rodgers, K. R. (1997) Characterization of ferrous FixL-nitric oxide adducts by resonance Raman spectroscopy, *Biochemistry 36*, 4178−4187.
40. Deinum, G., Stone, J. R., Babcock, G. T., and Marletta, M. A. (1996) Binding of nitric oxide and carbon monoxide to soluble guanylate cyclase as observed with resonance Raman spectroscopy, *Biochemistry 35*, 1540−1547.
41. Kitagawa, T., Kyogoku, Y., Iizuka, T., and Ikeda-Saito, M. (1976) Nature of the iron-ligand bond in ferrous low spin hemoproteins studied by resonance Raman scattering, *J. Am. Chem. Soc. 98*, 5169−5173.
42. Kitagawa, T., Nagai, K., and Tsubaki, M. (1979) Assignment of the Fe−N_ϵ (His F8) stretching band in the resonance Raman spectra of deoxy myoglobin, *FEBS Lett. 104*, 376−378.
43. Kincaid, J., Stein, P., and Spiro, T. G. (1979) Absence of heme-localized strain in T state hemoglobin: insensitivity of heme-imidazole resonance Raman frequencies to quaternary structure, *Proc. Natl. Acad. Sci. U.S.A. 76*, 549−552.
44. Johnson, W. C. (1999) Analyzing protein circular dichroism spectra for accurate secondary structures, *Proteins 35*, 307−312.
45. Sreerama, N., and Woody, R. W. (1993) A self-consistent method for the analysis of protein secondary structure from circular dichroism, *Anal. Biochem. 209*, 32−44.
46. Sreerama, N., and Woody, R. W. (1994) Poly(pro)II helices in globular proteins: identification and circular dichroic analysis, *Biochemistry 33*, 10022−10025.
47. Muller-Eberhard, U., and Nikkila, H. (1989) Transport of tetrapyrroles by proteins, *Semin. Hematol. 26*, 86−104.
48. Iwahara, S., Satoh, H., Song, D. X., Webb, J., Burlingame, A. L., Nagae, Y., and Muller-Eberhard, U. (1995) Purification, characterization, and cloning of a heme-binding protein (23 kDa) in rat liver cytosol, *Biochemistry 34*, 13398−13406.
49. Beaven, G. H., Chen, S. H., D'Albis, A., and Gratzer, W. B. (1974) A spectroscopic study of the haemin−human-serum-albumin system, *Eur. J. Biochem. 41*, 539−546.
50. Blackmon, B. J., Dailey, T. A., Lianchun, X., and Dailey, H. A. (2002) Characterization of a human and mouse tetrapyrrole-binding protein, *Arch. Biochem. Biophys. 407*, 196−201.
51. Ignarro, L. J., Ballot, B., and Wood, K. S. (1984) Regulation of soluble guanylate cyclase activity by porphyrins and metalloporphyrins, *J. Biol. Chem. 259*, 6201−6207.
52. Ogawa, K., Sun, J., Taketani, S., Nakajima, O., Nishitani, C., Sassa, S., Hayashi, N., Yamamoto, M., Shibahara, S., Fujita, H., and Igarashi, K. (2001) Heme mediates derepression of Maf recognition element through direct binding to transcription repressor Bach1, *EMBO J. 20*, 2835−2843.
53. Horio, Y., and Murad, F. (1991) Solubilization of guanylyl cyclase from bovine rod outer segments and effects of lowering Ca2+ and nitro compounds, *J. Biol. Chem. 266*, 3411−3415.
54. Kutty, R. K., Kutty, G., Wiggert, B., Chader, G. J., Darrow, R. M., and Organisciak, D. T. (1995) Induction of heme oxygenase 1 in the retina by intense visible light: suppression by the antioxidant dimethylthiourea, *Proc. Natl. Acad. Sci. U.S.A. 92*, 1177−1181.
55. Schwartzman, M. L., Masferrer, J., Dunn, M. W., McGiff, J. C., and Abraham, N. G. (1987) Cytochrome P450, drug metabolizing enzymes and arachidonic acid metabolism in bovine ocular tissues, *Curr. Eye Res. 6*, 623−630.

BI048742I